

DRYING AND CRACKING EFFECTS IN BOX-GIRDER BRIDGE SEGMENT

By Zdeněk P. Bažant, Fellow, ASCE,¹ Vladimír Krístek,² and Jan L. Vitek³

ABSTRACT: This paper deals with the effect of drying as a moisture diffusion process in a segment of a typical box-girder bridge. Pore relative humidity distributions throughout the cross sections of the plates of the girder are calculated from the diffusion equation, taking its nonlinearity and aging into account. The effect of creep with aging on the stresses produced by drying shrinkage is taken into account assuming a creep law based on the principle of superposition and described by an aging spring-dashpot chain model. The cross effects between creep and drying, expressed as stress-induced shrinkage (equivalent to drying creep), are considered. Tensile strain softening (smeared cracking) is taken into account in the form of an additive cracking strain. Localization of cracking and energetic fracture-mechanics aspects are neglected. A general algorithm for step-by-step integration in time is presented and verified by a convergence study. An example of analysis of the cross section of one recently built bridge confirms the feasibility of the analysis and indicates that the effect of the diffusion process of drying on the stress distributions is very large, in fact, so large that the stress values obtained by customary methods are merely fictitious.

INTRODUCTION

The long-time drying process, as well as temperature fluctuations, in concrete structures cause either tolerable or intolerable cracking. To ensure such damage would be tolerable, a more realistic method of analysis than those used in the current practice is needed. The current methods, based on codes and standard recommendations, generally do not yield adequate information on the stress and strain distributions produced by changes of moisture content or temperature. They are capable of furnishing only approximate, and sometimes quite inaccurate, values of normal forces and bending moments in the cross sections of beams and plates. These limitations are due mainly to the omission of moisture diffusion analysis and inadequacy of the simplified shrinkage and creep laws in use at present. These laws characterize only the overall behavior of the cross section, and especially ignore the diffusion aspects of the drying process. Properly, a material constitutive equation that describes the behavior of a small material element rather than the average response of the cross section should be used.

Free, i.e., unrestrained, shrinkage is an abstraction, nonexistent in reality. During the process of drying, as well as heating or cooling, the drop of moisture content or temperature occurs first in the surface layers and only much later in the core, as described by the solution of the diffusion equation for moisture transport. The material shrinkage and thermal expansion first develop in the surface layers. This produces tension in the surface layers, which must be balanced by compression in the core of the cross section. As

¹Walter P. Murphy Prof. Civ. Engrg., Northwestern Univ., Evanston, IL 60208.

²Prof. Civ. Engrg., Czech Tech. Univ., Prague, Czechoslovakia; formerly, Visiting Scholar, Northwestern Univ., Evanston, IL.

³Res. Engr., Czech Tech. Univ., Prague, Czechoslovakia.

Note. Discussion open until June 1, 1992. To extend the closing date one month, a written request must be filed with the ASCE Manager of Journals. The manuscript for this paper was submitted for review and possible publication on March 19, 1990. This paper is part of the *Journal of Structural Engineering*, Vol. 118, No. 1, January, 1992. ©ASCE, ISSN 0733-9445/92/0001-0305/\$1.00 + \$.15 per page. Paper No. 26538.

the drying process advances, the shrinkage- and temperature-induced stresses vary throughout the cross section. Because of irreversible strains due to distributed microcracking, as well as additional stress-induced shrinkage, the process does not end up with a uniform state of stress and strain. Rather, residual stresses remain.

Intense research has now finally crystallized into a material model that ought to give a realistic picture of stresses and strains in concrete structures exposed to drying and temperature changes. After a period of development of realistic constitutive relations for shrinkage and basic creep of concrete ("State" 1988; Bažant and Panula, 1978), two advances that seem to complete the requisite material model have recently been made: (1) The constitutive relation for creep has been extended to also cover the cross effects with shrinkage and thermal strains, known as either stress-induced shrinkage or drying creep, and as stress-induced thermal strain [e.g., Bažant (1972), Thelandersson (1983), Bažant and Chern (1985a, 1985b)]; and (2) the law that governs the strain softening due to distributed tensile cracking has been formulated and verified experimentally [e.g., ACI Committee 446, (1991), Bažant (1986)].

The objective of this paper is to apply the aforementioned advances in material modeling to the problem of drying effects in the cross section of a segment of a prestressed concrete box-girder bridge (Fig. 1). A numerical example of the cross section of one recently completed bridge will be used to examine the effects of drying from the designer's viewpoint and to demonstrate the feasibility of this type of analysis in practice.

MATERIAL MODEL AND GOVERNING EQUATIONS

Diffusion and Aging

Prior to the solution of stresses, it is necessary to calculate the distributions of pore relative humidity, h , as well as temperature through the entire structure at various times. We will assume the pore humidity and temperature to be governed by uncoupled diffusion equations. The uncoupling appears to be an acceptable approximation, unless the cracks open widely (Bažant et al. 1988) or the moisture and temperature gradients are high (Bažant and Thonguthai (1979), which is not normally the case. We will further assume that the moisture movement is one-dimensional, occurring only in the directions normal to the plates of the cross section, i.e., we will neglect moisture migrations along the plates and in the longitudinal direction of the girder. The pore relative humidity as a function of time t and of the

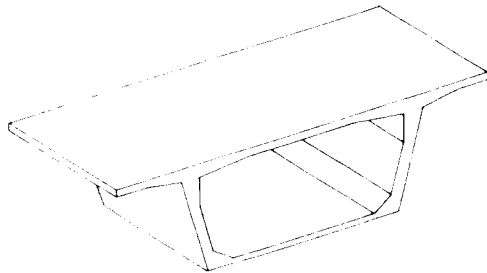


FIG. 1. Box Girder Bridge Segment Analyzed

transverse cross section coordinate z of the walls is governed by the following nonlinear parabolic partial differential equation:

$$\frac{\delta h}{\delta t} = \frac{\delta}{\delta z} \left[C(t, h) \frac{\delta h}{\delta z} \right] \dots \dots \dots (1)$$

The boundary conditions consist of prescribed values of h representing the environmental conditions. The diffusivity, $C(t, h)$, is variable, due to aging of concrete. It depends not only on time, but also on the local moisture content, which is a function of h . The dependence of C on h is very strong and may be approximately described by the following empirical (but physically explicable) equation (Bažant and Najjar 1972; "State" 1988):

$$C(t, H) = C_i(t_i) \left[\alpha_0 + \frac{1 - \alpha_0}{1 + \frac{(1 - h)^n}{(1 - h_c)^n}} \right] \dots \dots \dots (2)$$

in which $C_i(t_i)$ = reference diffusivity of moisture in concrete at full saturation ($h = 1$), which depends on the equivalent hydration period, t_i ; and α_0 , n , and h_c = empirical constants, $\alpha_0 \approx 0.05$, $h_c \approx 0.75$, $n \approx 6$. Furthermore (Bažant 1975; Bažant and Chern 1985a):

$$C_i(t_i) = C_0(0.3 + 3.6t_i^{-1.2}) 10^{-6} \quad (\text{m}^2/\text{day}) \dots \dots \dots (3)$$

in which t_i must be given in days; and C_0 = an empirical constant, roughly representing the diffusivity at saturation at 28 days of age, typically $C_0 \approx 0.1 \text{ cm}^2/\text{day}$. The evolution of the equivalent hydration period reflects the effect of pore humidity and temperature on the local rate of cement hydration. It may be approximately characterized by the equation

$$t_i = \int_0^t \phi_h(t') \phi_T(t') dt' \dots \dots \dots (4)$$

in which

$$\phi_h = 0.5(1 + h^2) \dots \dots \dots (5)$$

$$\phi_T = \exp \left(\frac{Q}{RT_0} - \frac{Q}{RT} \right) = \exp \left(\frac{5000}{T_0} - \frac{5000}{T} \right) \dots \dots \dots (6)$$

Here t' = age of concrete; Q = activation energy; R = gas constant; T = absolute temperature (in degrees K); and T_0 = reference temperature (in degrees K), usually taken at 20° C.

The diffusion equation for heat conduction is simpler than that for humidity since the heat diffusivity, a , can be considered to be approximately constant;

$$\frac{\delta T}{\delta t} = a \frac{\delta^2 T}{\delta z^2} \dots \dots \dots (7)$$

It must be admitted that the values of moisture diffusivity are also affected by concrete cracking (Bažant et al. 1988), but this dependence is significant only if cracks wider than about 0.2 mm develop, which we assume will not occur. The strain and stress of concrete has no appreciable effect on C . Therefore, the problem of pore humidity as well as temperature distribution

can be approximately considered to be uncoupled from the stress-deformation problem and can be solved separately, in advance. This makes the computer solution by finite elements or finite differences relatively easy.

Shrinkage, Thermal Strain and Creep

The free shrinkage strain of concrete, ϵ_s , which is an abstraction and is not directly measurable in the laboratory, can be approximately described as [e.g., "State" (1988), Bažant and Wang (1985)]:

$$\epsilon_s = \kappa(1 - h^3) \dots \dots \dots (8)$$

in which κ = an empirical constant, generally between -0.0002 and -0.0010 , and is here taken as $\kappa = -0.0008$. The free temperature expansion (dilatation) is incrementally defined by the well-known relation:

$$\Delta\epsilon_T = \alpha_T \Delta T \dots \dots \dots (9)$$

in which Δ refers to a change during the time step of computation; and α_T = thermal expansion coefficient, taken as $1.2 \times 10^{-5} K^{-1}$.

A peculiar but essential property of the hygrothermal properties of concrete is the existence of large additional creep strains, called the drying creep and the transitional thermal creep, which depend on \dot{h} and \dot{T} (Bažant 1972). As an approximation, it is convenient to treat these additional strains as stress-induced shrinkage, ϵ_{CS} , and stress-induced thermal expansion, ϵ_{CT} . They are incrementally described by the equations (Bažant and Chern 1985a, 1985b):

$$\Delta\epsilon_{CS} = -\kappa r g_h \sigma \Delta h, \quad \Delta\epsilon_{CT} = -\alpha_T \rho g_T \sigma \Delta T \dots \dots \dots (10)$$

in which $g_h = 1$ if $\dot{h} \geq 0$, $g_h = -1$ if $\dot{h} < 0$; $g_T = 1$ if $\dot{T} \geq 0$, $g_T = -1$ if $\dot{T} < 0$; σ = uniaxial stress; and r, ρ = empirical coefficients normally having the values of $r = (0.1-0.6)f'_c \text{ MPa}^{-1}$, $\rho = (1-2)f'_c \text{ MPa}^{-1}$.

The stresses produced by nonuniform shrinkage and thermal expansion, along with the stress-induced shrinkage and thermal strain, cause elastic deformations and creep. In the present study, the basic compliance function for creep is taken in the form of the triple power law, in a form roughly equivalent to the BP model for basic creep (Bažant and Panula 1978; "State" 1988). It may be noted that the subsequently developed solidification theory for basic creep (Bažant and Prasanna 1989) is both more realistic and more convenient for calculations; however, in the present problem, the difference would be insignificant. The drying creep is not included in the compliance function because it is taken into account separately in the form of stress-induced shrinkage.

The analysis of the structure is carried out numerically by finite elements, in small time steps Δt . For this purpose, the stress-strain relation with creep is assumed to follow the principle of superposition, and is approximated according to a rheologic spring-dashpot chain model [see "State" (1988)]. Such an approximation generally yields the incremental stress-strain relation for creep and elastic deformations of concrete during each time step in the form:

$$\Delta\epsilon = \frac{\Delta\sigma}{E''} + \Delta\epsilon'' \dots \dots \dots (12)$$

in which $\Delta\sigma$ and $\Delta\epsilon$ = the increments of stress and strain during the time step; and E'' = incremental pseudoelastic modulus that reflects both elastic

and creep deformations. In each time step, E'' is calculated as described in Bažant and Chern (1985a, 1985b) or Bažant (1982b). $\Delta\epsilon''$ = inelastic strain increment during the time step, which is expressed as:

$$\Delta\epsilon'' = \Delta\epsilon_C + \Delta\epsilon_S + \Delta\epsilon_T + \Delta\epsilon_{CS} + \Delta\epsilon_{CT} + \Delta\xi \dots \dots \dots (13)$$

Here ξ is the cracking strain, which will be characterized later. The fact that this strain is additive to the other inelastic strains is an important hypothesis of the present formulation, justified in Bažant and Chern (1985a, 1985b). $\Delta\epsilon_C$ is the creep strain increment caused by all the stress increments that arose in the preceding time intervals.

The values of E'' are different at various points of the structure, even if the concrete properties are homogeneous. In this study, the values of $\Delta\epsilon''$ and E'' were calculated on the basis of the Maxwell chain model, in the manner described [e.g., in "State" (1988), or Bažant (1982b)]. In retrospect, though, it must now be admitted that it would have been better to calculate $\Delta\epsilon''$ on the basis of the subsequently developed solidification theory (Bažant and Prasanna 1989), in which the creep is modeled, in transformed time, by a nonaging Kelvin chain model and all the aging effect is introduced by another, physically motivated, transformation of time. However, for the results of the present calculations this would not make a significant difference.

Cracking Strain and Strain Softening

Nonuniform drying as well as temperature changes typically produce strains that exceed the maximum stress state and engender microcracking, macroscopically manifested as strain softening. The microcracks may further grow and coalesce into continuous cracks; or they may later close, in which case, compression stresses can be transmitted across the cracks. Redistribution of internal forces tends to localize microcracking in isolated portions of a statically indeterminate structure. The bending and axial stiffnesses of the cross section are reduced by microcracking.

In a smeared continuous description, cracking is taken into account by a stress-strain diagram that exhibits strain softening [Fig. 2(a)]. The peak stress value is the tensile strength, f'_t . For the purpose of creep calculations, it is convenient to subtract from the strains in Fig. 2(a) the elastic strains corresponding to the same stress. This yields the stress-strain diagram in Fig. 2(b), which involves only that portion of strain (denoted as ξ) which is due to smeared cracking and has already appeared in (13). It may be described by the formula (Bažant and Chern 1985b):

$$\sigma = B \xi^q e^{-c\xi} = C(\xi)\xi = f(\xi) \dots \dots \dots (13)$$

B, q, c , and s = empirical constants that depend on the tensile strength and the strain at peak stress; and $C(\xi) = B\xi^{q-1} \exp(-c\xi) = \text{secant modulus}$.

Fig. 2(b) illustrates only the response at monotonically increasing tensile strain. If the strain begins to decrease, as illustrated in Fig. 2(c), the microcracks are closing but cannot close fully due to previous creation of fragments on the microcrack surfaces. Therefore, unloading does not return the response to the origin but leads to compressive stresses at positive strains [Fig. 2(c)]. Following Bažant and Chern (1985a), the stress-strain relation for unloading is defined incrementally as

$$\Delta\sigma = C(\xi) \Delta\xi \dots \dots \dots (14)$$

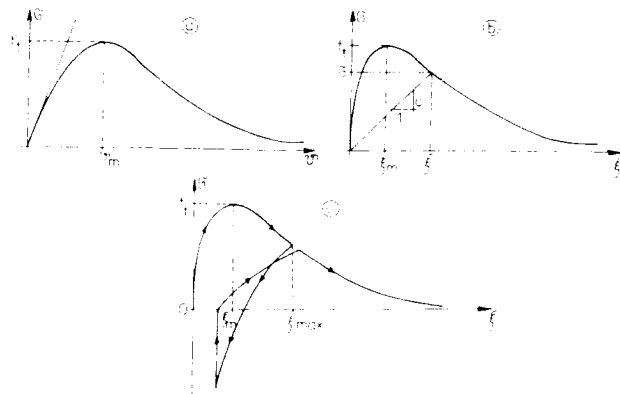


FIG. 2. (a) Stress-Strain Diagram of Concrete in Tension; (b) Diagram of Stress versus Cracking Strain ξ ; and (c) Variation of Cracking Strain Assumed for Unloading and Reloading

For the stress-strain diagram at reloading, two cases are distinguished.

1. The stress is compressive. It is assumed that removal of the compressive strain causes no cracking strain, and, therefore, the stress-strain diagram is vertical up to the strain axis, as shown in Fig. 2(c).

2. The stress is tensile. In this case, the microcracks have not quite closed during previous unloading, and they start reopening at reloading. It is assumed that the tangent cracking stiffness \bar{C} is the average of the secant stiffness for the current cracking strain ξ on the virgin loading diagram and the secant stiffness for the maximum previous cracking strain, i.e.,

$$\Delta\sigma = \bar{C}(\xi)\Delta\xi, \quad \bar{C}(\xi) = \frac{1}{2} [C(\xi) + C(\xi_{\max})] \dots\dots\dots (15)$$

When the reloading diagram reaches again the virgin loading diagram, further behavior is described by the virgin loading diagram [Fig. 2(c)].

In the foregoing formulation for creep, we assume that the cracking (strain-softening) part of strain, ξ , is not time-dependent. This is almost certainly a simplification. Recent tests in progress at Northwestern University indicate that the relative creep (per unit stress) in the strain-softening fracture process zone is several times larger than that for the same stress in the hardening (prepeak) regime. On the other hand, it is not clear whether such a property of fracture process zone needs to be considered when strain softening is not localized.

Other Aspects

Strain softening is known to be prone to localization instabilities, in which case the structure needs to be analyzed according to nonlinear fracture mechanics or some nonlocal continuum model. In the present study we assume that no localization instabilities or localized fractures develop. This assumption seems to be usually adequate for cracking in flexure of strongly reinforced beams, in which the localization of cracking into major fractures

is prevented by both the reinforcement and the restraining effect of the compression zone of concrete in the beam (Bažant and Oh 1983).

We also neglect in the present formulation the effect of random fluctuation of environmental humidity. Eventually, a realistic analysis would have to take this effect into account, but the probabilistic approach required is still being researched (Bažant and Xi 1989). On the other hand, calculation of the effects of the random nature of material properties as well as the errors of the constitutive model is by now relatively well understood [e.g., Tsubaki et al. (1988)] and could be incorporated into the present analysis if this were not beyond the scope of a single paper.

The present material model has previously been verified and calibrated by a large number of test data, including those of Thelandersson (1983), Troxell et al. (1958), L'Hermite et al. (1965), McDonald (1975), Brooks and Neville (1977), Ward and Cook (1969), Pickett (1942), Ruetz (1966), Glücklich and Ishai (1962), Hanson (1953), Wittmann and Roelfstra (1980), Petersson (1981), Reinhardt and Cornelissen (1984), and Gopalratnam and Shah (1984).

NUMERICAL STRUCTURAL ANALYSIS

For two-dimensional deformations in the plane of the cross section of the girder, the bridge segment may be treated as a frame in which the plates of the cross section represent beams. The beams are subdivided into beam finite elements, each of which is further subdivided into a number of layers. Some of the layers are used to represent the steel reinforcement, which is assumed to remain elastic. Bond slip is neglected. The cross sections of the beams are assumed to remain plane and normal to the deflection line. The solution is accomplished in small time steps.

Since the moisture diffusion is treated as one-dimensional in the direction across the plate (beam), the solution for given boundary conditions of humidity and temperature is obtained independently within each cross section, using Crank-Nicolson finite difference algorithm [see e.g., Bažant and Najjar (1972)]. This yields, in advance of stress analysis, the values of pore relative humidity and temperature at the centroid of each layer of each cross section, at each discrete time.

An effective general step-by-step algorithm for calculating the stresses, deflections, and strains was developed by Bažant and Chern (1985b). Although this algorithm could be applied to the present problem, a slightly different but similar algorithm, which compromises some efficiency for simplicity of programming, has been formulated and used in the present problem. In each time step (t_{r-1}, t_r), the solution proceeds as follows.

1. Solve the values of Δh , ΔT for the centroid of each layer in each cross section, and set $h_{r+1} = h_r + \Delta h$, $T_{r+1} = T_r + \Delta T$ (subscript r refers to time t_r). Then, using the values of the partial stresses or partial strains in the rheologic model at time t_r , calculate the values of E'' and $\Delta \epsilon_c$ for the centroid of each layer of each cross section [as described, e.g., in Bažant (1982a)].
2. Start iteration loop.
3. Calculate $\Delta \epsilon_s$, $\Delta \epsilon_T$, $\Delta \epsilon_{cs}$, and $\Delta \epsilon_{cT}$ for the centroid of each layer in each discrete cross section, using the values of Δh , ΔT and $\bar{\sigma} = \sigma_r + \Delta\sigma'/2$ where, for the first iteration, $\Delta\sigma' = 0$, and for the subsequent iterations, $\Delta\sigma' =$ value of $\Delta\sigma$ obtained in the previous iteration of this time step.
4. For the centroid of each layer of each cross section, decide whether there

is loading, unloading, or reloading: (A) If there is loading, use $\Delta\xi = 0$ for the first iteration, and for the subsequent iterations solve $\Delta\xi$ from the nonlinear equation $f(\xi_i + \Delta\xi) = \sigma_i + \Delta\sigma_i$, which can be effectively accomplished by Newton iterations; (B) if there is unloading or reloading, use $\Delta\xi = \Delta\sigma C(\xi)$, where $\xi = \xi_i + \Delta\xi_i$; for the first iteration $\Delta\xi_i = 0$ while for the subsequent iterations $\Delta\xi_i =$ value of $\Delta\xi$ obtained in the previous iteration. Then calculate the total inelastic strain increment $\Delta\varepsilon''$.

5. Imagining the end cross sections of every beam element to be temporarily fixed (frozen), calculate the inelastic stresses $\Delta\sigma'' = E'' \Delta\varepsilon''$. Then evaluate the axial and bending resultants $\Delta N''$ and $\Delta M''$ for each discrete cross section.

6. Imagine the cross sections to be released (unfrozen). This is equivalent to applying on the end cross sections of the beam elements axial internal forces $-\Delta N''$ and bending moments $-\Delta M''$. Then calculate the external loads (transverse and axial distributed loads) Δp^* and Δq^* , which are in equilibrium with $-\Delta N''$ and $\Delta M''$. Add Δp^* and Δq^* to the prescribed changes Δp , Δq of applied loads, and solve the elastic structure considering its elastic moduli to be E'' (which are in general different in each layer of each cross section). This yields the increments Δw , $\Delta\varepsilon$, and $\Delta\sigma$ of deflections, strains and stresses in the structure.

7. Check for convergence by calculating the ratio $R = \sum_i |\Delta w_i - \Delta\bar{w}_i| / \sum_i |\Delta w_i|$ where subscript i ($= 1, 2, \dots, n$) refers to all the discrete cross sections and Δw_i , $\Delta\bar{w}_i$ are the deflection increments obtained in this iteration and in the preceding iteration, respectively. If $R >$ given small tolerance (e.g., 0.005), go to step 2 and start the next iteration of this step. Otherwise go to 1 and start the next time step.

Note that the Newton iterations for ξ could be eliminated from the foregoing algorithm if (13) could be explicitly inverted.

The fact that (13) yields a horizontal tangent at the peak stress point may cause numerical difficulties for states at or very near the peak point. Their accurate handling would necessitate a more sophisticated algorithm (e.g., the arc-length method known from nonlinear finite element analysis). However, for practical purposes where high accuracy is not necessary, numerical difficulties can be avoided just by taking a larger time step that straddles the peak point of the $\sigma(\xi)$ diagram.

In the numerical example that follows, only the effect of drying will be analyzed, for the sake of simplicity. However, the effect of temperature changes could be analyzed in an analogous manner.

EXAMPLE: BOX GIRDER BRIDGE

As an example, we now present the analysis of the behavior of the cross section of the Kishwaukee River Bridge in Illinois, shown in Fig. 3(a). The longitudinal reinforcement and prestress of the girder is assumed to have no effect in the present analysis. The cross section is reinforced by mild steel [Fig. 3(a)]. The girder is assembled from precast segments, and we analyze the behavior of one segment in the transverse plane, assuming two-dimensional response and plane strain conditions. The segment is cured in the formwork and at the age of seven days, the formwork is stripped. At that moment, the drying of concrete begins and the own weight begins to act.

The effects of the fluctuations of environmental humidity and temperature are neglected in this example. Their realistic analysis would necessitate a

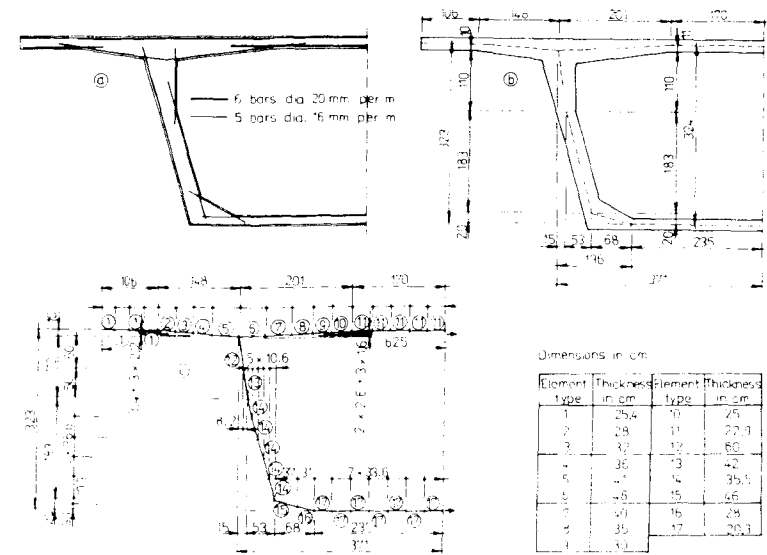


FIG. 3. (a) Reinforcement of Box Girder in Cross-Section Plane; (b) Subdivision in Finite Elements; and (c) Geometry of Neutral Axis

probabilistic approach that takes into account the randomness of the process (Bažant and Wang 1984a, 1984b; Bažant and Xi 1989).

After stripping, the surfaces of concrete are exposed to the environmental humidity, which is considered to be $h = 0.5$ on the outside and 0.6 on the inside of the box. The reason for assuming the average humidity at the inner surface to be higher than at the outer surface is that the interior space is not as well ventilated as the exterior space and is not illuminated by sun. So the bridge segment loses moisture faster to the outside than to the inside.

As the boundary condition for the diffusion equation of drying, the pore relative humidities at the exterior and interior surfaces of the cross section plates are assumed to approach the environmental values gradually, as shown in Fig. 4. This assumption does not describe the ideal situation of a structure suddenly exposed to an environment of constant controlled relative humidity, as in the laboratory. Rather, this assumption is intended to approximately reflect field conditions. After the stripping of the form, a box-girder segment is still subjected for some time to periodic, although perhaps sporadic, moist treatment. This causes the average daily relative humidity at the surface of concrete to approach the average environmental humidity with a considerable delay rather than immediately. If the ideal conditions of a sudden drop of surface humidity to its constant environmental value were considered, the effects of drying would be more severe than those calculated in this paper.

For the purpose of analysis, the plates of the cross section are subdivided into finite elements as shown in Fig. 3(b). Each finite element is subdivided into 14 equally thick layers. The geometry of the neutral axis of the beam elements is shown in Fig. 3(c).

We analyze the deformations of the cross section and the stresses caused by drying during a period of 55 days after stripping. The period from strip-

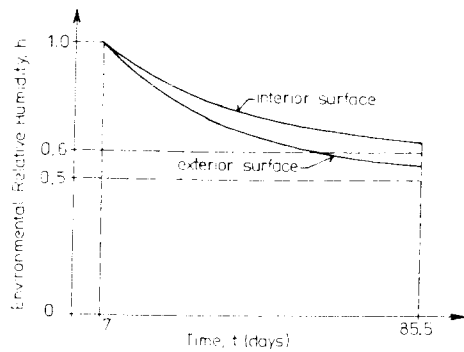


FIG. 4. Assumed Variation of Relative Humidity at Interior and Exterior Surfaces of Plates of Cross Section

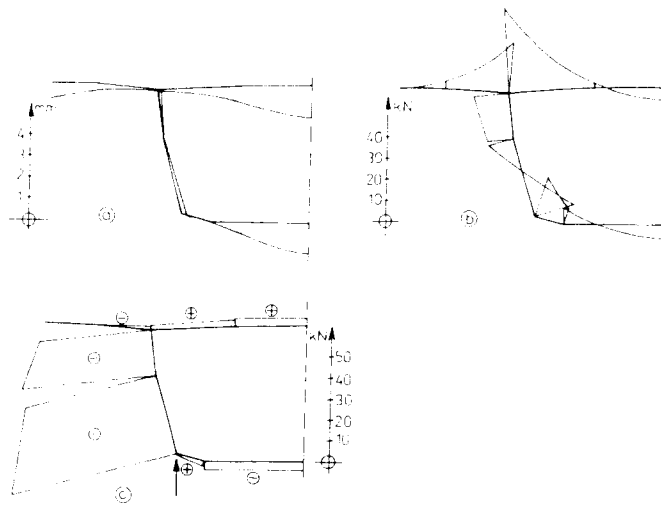


FIG. 5. (a) Calculated Deformation of Cross Section; (b) Distribution of Bending Moments; (c) Distribution of Normal Forces

ping to joining of the segment with its neighbors may sometimes be as long as this.

Fig. 5(a) shows exaggerated deformation of the cross section at the final time (55 days after stripping). The cross section is assumed in the analysis to be simply supported at the bottom corners of the box. Obviously, the major part of deflections is caused by own weight. The drying shrinkage of concrete is manifested principally by shortening of the distance between the opposite plates, which is, however, relatively small compared to transverse deflections of the plates.

Fig. 5(a) shows the distribution of the bending moments at the final time. As we see, their maxima arise at the upper corners at which the top plates and the web join. The moments caused by nonuniformity of shrinkage are

not particularly manifested in Fig. 5(b). The final distribution of the normal forces in the plates of the cross section is shown in Fig. 5(c). Again the effect of own weight dominates, and even the small tensile force in the bottom plate seems to be caused by the transmission of the own weight component from the web to the bottom plate.

The final distributions of the normal stresses in the axial directions are shown for several typical cross sections in Figs. 6(a-d). In contrast to the bending and axial internal force resultants in the cross sections, the stress distribution is strongly influenced by nonuniform drying as well as strain softening. Even in regions where the usual analysis without drying would indicate compression, significant tensile stresses arise due to shrinkage. The stresses in steel in the compressed zones reach values around 20 MPa. In these distributions, one can clearly see the effect of strain softening due to microcracking, which causes the drop of stress near the surfaces. The largest compression stresses are reached in the bottom plate, which is the thinnest (see the distribution for element 33); the reason is that the tensile stresses produced by drying in the surface layers are counteracted in compression by concrete of a smaller thickness than in the other plates. This is also the reason why the axial shrinkage in the bottom plate is the largest.

For comparison purposes, the alternative case, in which the segment is without reinforcement, is free from own weight, and is affected only by drying has also been solved. Fig. 7(a) shows the final deformation of the cross section due to shrinkage. The bottom plate shrinks more than the upper plate because it is thinner. This difference in shrinkage causes the distribution of axial forces shown in Fig. 7(b), and the distribution of bending moments, shown in Fig. 7(c). The bending moments are produced by the

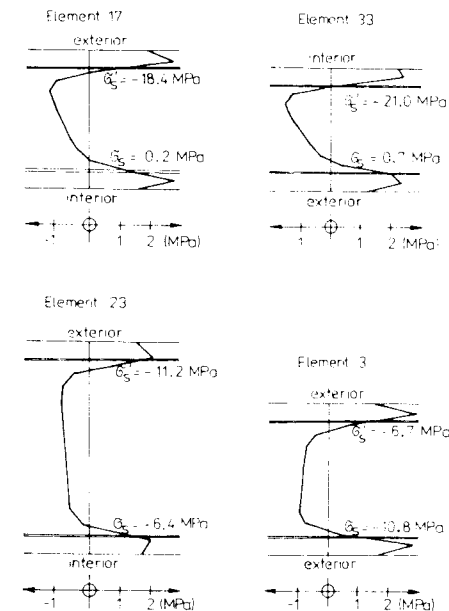


FIG. 6. Calculated Stress Distributions Over Cross Sections of Four Finite Elements in Box

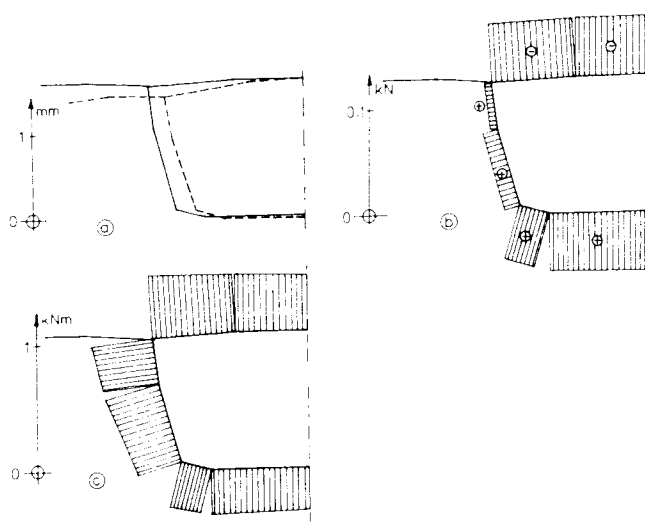


FIG. 7. Effects of Drying, Own Weight Neglected; (a) Deformation of Cross Section; (b) Distribution of Normal Forces; (c) Distribution of Bending Moments

axial force resultants due to nonuniform shrinkage and the associated nonuniform shortening of the neutral axis. The maximum bending moments arise at the joint of web and upper plate, at which the plate thicknesses are the largest. Fig. 8 shows the final stress distributions, which are quite similar to those obtained when the own weight is taken into account (Fig. 6). The stress distribution in element 3 of Fig. 8 is seen to be nearly symmetric, which is due to the fact that both surfaces of the cantilever plate are exposed to the same humidity. The other stress distributions show a mild nonsymmetry, which appears to be due mainly to the small differences in relative humidities considered for the opposite surfaces.

CONVERGENCE OF NUMERICAL ALGORITHM

The present numerical algorithm has been verified by checking the convergence as the subdivision of time or space is refined.

Effect of Plate Subdivision into Layers

To study this effect, only one finite element, which is either fixed or free at both ends, has been analyzed. These boundary conditions are the extreme cases of real situations. The number of layers has been varied from 6 to 48, considering a plate of thickness 200 mm. For the integration in time, the test duration of 0.25 year was considered, and this duration was subdivided into 6 to 48 time intervals of equal length. The effect of these subdivisions on the axial normal force in the element and on the bending moment is shown in Figs. 9 and 10. One can see that the results appear to converge and that the differences between the last two subdivisions are minimal. It may also be noted that the normal force converged faster than the bending moment.

For the cases of fixed and free finite elements of the plate, the convergence

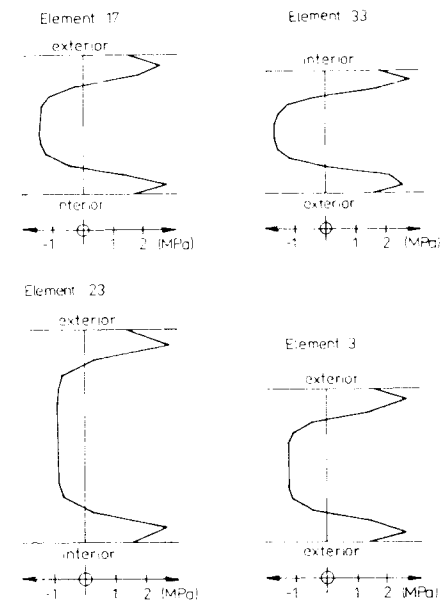


FIG. 8. Stress Distributions Over the Cross Sections of Four Elements, Caused by Drying, Own Weight Neglected

of the stresses at the surfaces and at the midthickness was also studied. It has been found that a subdivision of the plate thickness into more than 14 layers does not yield any appreciable change in the results. On the other hand, the subdivision of time has a large effect on the stress distributions and needs to be dense, while for the cross section resultants of bending moment and axial force as well as the overall shortening, a cruder subdivision of time is sufficient. It has also been noted that the convergence of stresses at points where their values are the largest is faster than at points where they are small. It has been concluded that a subdivision of thickness into 14 layers and time intervals of 3 days are sufficient. [Computationally, however, it would have been more effective to use time intervals that increase with time; see ACI Committee 466, (1989).]

Effect of Subdivision into Finite Elements

This effect was studied on a beam fixed at one end and simply supported at the other end. The beam was exposed to different surface humidities on top and bottom, as already mentioned. Aside from the shortening of the segment, the nonsymmetric humidities also cause curvature. Due to redundancy of the beam, shrinkage produces end reactions. The beam is subdivided into 3, 6, 9, and 12 finite elements. The response is calculated for the time of 0.25 year after the start of drying, at which the age of concrete is 7 days. Each finite element is subdivided into 14 layers. Calculations revealed that the differences due to the aforementioned element subdivisions are rather small. This is illustrated by Fig. 10(a), which shows the dependence of the bending moments at two cross sections of the beam on the number of finite elements. The corresponding stress distribution at midspan is shown in Fig. 10(b).

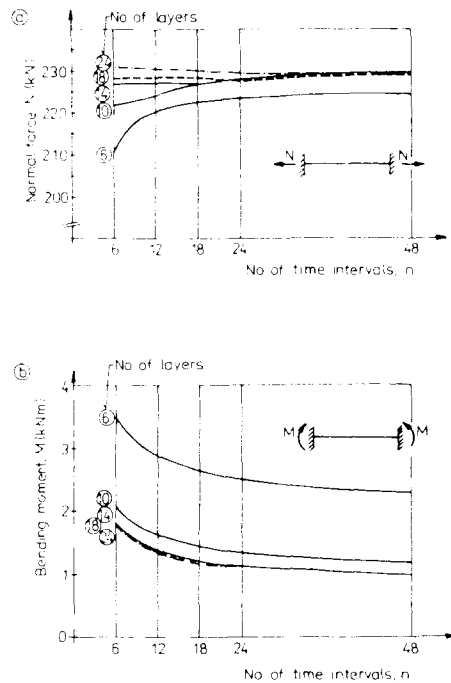


FIG. 9. Convergence with Refinement of Time Subdivision: (a) Normal Force; (b) Bending Moment

The convergence study confirms the validity of the numerical algorithm used and indicates that the discretization errors are acceptable.

CONCLUSIONS

1. The present study confirms the feasibility of analyzing box-girder bridges for: (A) The effect of the diffusion nature of the drying process; (B) the effects of creep (with aging), which significantly reduce the stresses due to drying shrinkage; (C) the effect of the additional stress-induced shrinkage (also called drying creep); (D) the effect of strain softening, which greatly reduces the shrinkage stresses. (Possible localization of strain softening and fracture mechanics aspects are neglected in this study.)

2. The effect of nonuniform drying, as described by the diffusion problem of moisture transfer through the pores of concrete, is very large, and greatly alters the stress distributions. The effect is so large that the stresses obtained by the usual analysis, which ignores diffusion phenomena, stress-induced shrinkage, and strain softening, are merely fictitious.

3. The convergence of the present algorithm with respect to subdivision of time, subdivision of beams into finite elements and subdivision of finite elements into layers is satisfactory. Although this algorithm is similar to that developed and verified previously (Bažant and Chern 1985b), it is more general in that it

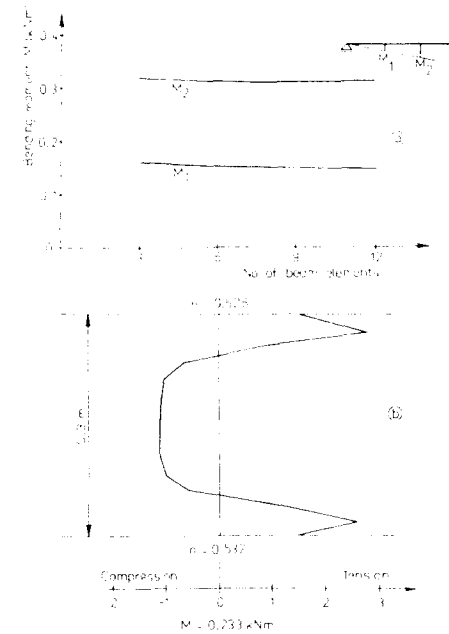


FIG. 10. Convergence when Element Subdivision of Beam is Refined: (a) Convergence of Bending Moments at Two Locations; (b) Corresponding Stress Distribution at Midspan for Finest Element Subdivision

allows incorporation of strain-softening effects into any algorithm for concrete creep, not just the exponential algorithm used before.

ACKNOWLEDGMENT

Partial financial support under NSF Grant number MSM-8815166 to Northwestern University is gratefully acknowledged.

APPENDIX. REFERENCES

- Bažant, Z. P. (1972). "Thermodynamics of interacting continua with surfaces and creep analysis of concrete structures." *Nucl. Engng. Des.*, 20, 477-505.
- Bažant, Z. P. (1975). "Theory of creep and shrinkage in concrete structures: a precis of recent developments." *Mechanics today*, Vol. 2, Pergamon Press, New York, N.Y., 1-93.
- Bažant, Z. P. (1982a). "Input of creep and shrinkage characteristics for a structural analysis program." *Materials and Structures, Research and Testing (RILEM, Paris)*, 15(88), 283-90.
- Bažant, Z. P. (1982b). "Mathematical models for creep and shrinkage of concrete." *Creep and shrinkage in concrete structures*, Z. P. Bažant and F. H. Wittmann, eds., John Wiley and Sons, London, England, 163-256.
- Bažant, Z. P. (1986). "Mechanics of distributed cracking." *Appl. Mech. Reviews*, 39, 675-705.
- Bažant, Z. P., and Chern, J.-C. (1985a). "Concrete creep at variable humidity: Constitutive law and mechanism." *Materials and Structures (RILEM, Paris)*, 18, 1-20.

- Bazant, Z. P., and Chern, J.-C. (1985b). "Strain softening with creep and exponential algorithm." *J. Engrg. Mech.*, ASCE 111(3), 391-415.
- Bazant, Z. P., and Chern, J.-C. (1987). "Stress-induced thermal and shrinkage strains in concrete." *J. Engrg. Mech.*, ASCE, 113(10), 1493-1511.
- Bazant, Z. P., and Najjar, L. J. (1972). "Nonlinear water diffusion in nonsaturated concrete." *Materials and Structures (RILEM, Paris)*, 5, 3-20.
- Bazant, Z. P., and Oh, B. H. (1984). "Deformation of progressively cracking reinforced concrete beams." *ACI J.* 81, 226-278.
- Bazant, Z. P., and Panula, L. (1978). "Practical prediction of time-dependent deformations of concrete." *Materials and Structures (RILEM, Paris)*, 11(65), 307-28, (66), 415-34; and 12(69), (1979), 169-83.
- Bazant, Z. P., and Prasanna, S. (1989). "Solidification theory for concrete creep: I. Formulation, and II. Verification and application." *J. Engrg. Mech.*, ASCE, 115(8), 1691-1725.
- Bazant, Z. P., Sener, S., and Kim, J. K. (1987). "Effect of cracking on drying permeability and diffusivity of concrete." *ACI Mater. J.*, 84(Sept), 351-357.
- Bazant, Z. P., and Wang, T.-S. (1984a). "Spectral analysis of random shrinkage stresses in concrete." *J. Engrg. Mech.*, ASCE, 110, 173-186.
- Bazant, Z. P., and Wang, T. S. (1984b). "Spectral finite element analysis of random shrinkage in concrete." *J. Struct. Engrg.*, ASCE, 110, 2196-211.
- Bazant, Z. P., and Xi, Y. (1989). "Probabilistic prediction of creep and shrinkage in concrete structures: combined sampling and spectral approach." *Proc., 5th Int. Conf. on Struct. Safety and Reliability (ICOSSAR)*, Vol. I, A. H.-S. Ang et al., eds., held in San Francisco, Published by ASCE, New York, N.Y. 803-808.
- Brooks, J. J., Neville, A. M. (1977). "A comparison of creep, elasticity and strength of concrete in tension and in compression." *Mag. Concr. Res.* 29(100), 131-141.
- ACI Committee 446 (1991), "Fracture mechanics of concrete: Concepts, models and determination of material properties." *ACI 446.1R-XX (state-of-art report)*, American Concrete Institute (ACI), Detroit, Mich.
- Glucklich, J., and Ishai, O. (1962). "Creep mechanism in cement mortar." *J. Am. Concr. Inst.*, 59, 923-948.
- Gopalaratnam, V. S., and Shah, S. P. (1985). "Softening response of concrete in direct tension." *ACI J.*, 81, May-Jun., 310-323.
- Hanson, J. A. (1953). "A ten year study of creep properties of concrete." *Concr. Lab. Report No. Sp-38*, U.S. Dept. of the Interior, Bureau of Reclamation, Denver, Colo.
- L'Hermite, R. G., Mamillan, M., Lefèvre, C. (1965). "Nouveaux résultats de recherches sur la déformation et la rupture du béton." *Annales de l'Institut Techn. du Bâtiment et des Travaux Publics*, 18(207-208) 325; see also *Int. Conf. on the Structure of Concrete, Cement and Concrete Association*, London, 1968, 423.
- McDonald, J. E. (1975). "Time dependent deformation of concrete under multiaxial stress conditions." *Tech. Report C-75-4*, U.S. Army Engrg. Waterways Experiment Sta., Vicksburg, Miss.
- Petersson, P. E. (1981). "Crack growth and development of fracture zones in plain concrete and similar materials." *Report TVBM 1006*, Lund Inst. of Tech., Lund, Sweden.
- Pickett, G. (1942). "The effect of change in moisture content on the creep of concrete under a sustained load." *J. Am. Concr. Inst.*, 47, 165-204, 361-397.
- Reinhardt, H. W., and Cornelissen, H. A. W. (1984). "Post-peak cyclic behavior of concrete in uniaxial tensile and alternating tensile and compressive loading." *Cem. Concrete Res.*, 14, 263-270.
- Ruetz, W. (1966). "A hypothesis for the creep of hardened cement paste and the influence of simultaneous shrinkage." *Int. Conf. Struct. of Concrete*, held in London, 1965, Cement and Concrete Association, London, United Kingdom, 1968, pp. 365-387, see also Deutscher Ausschuss für Stahlbeton, Heft 183, 1966.
- "State of the art in mathematical modeling of creep and shrinkage of concrete" (by RILEM Committee TC69) (1988). *Mathematical modeling of creep and shrinkage of concrete*, Z. P. Bazant, ed., J. Wiley and Sons, New York, N.Y., 57-392.
- Thelandersson, S. (1983). "On the multiaxial behavior of concrete exposed to high temperature." *Nucl. Engrg. Des.*, 75(2), 271-82.
- Troxell, G. E., Raphael, J. M., Davis, R. W. (1958). "Long-time creep and shrinkage tests of plain and reinforced concrete." *Proc. ASTM*, 58, 151-158.
- Tsubaki, T. et al. (1988). "Probabilistic models." *Mathematical modeling of creep and shrinkage of concrete*. Z. P. Bazant, ed., J. Wiley and Sons, New York, N.Y., 311-383.
- Ward, M. A., Cook, D. J. (1969). "The mechanism of tensile creep in concrete." *Mag. Concr. Res.*, 21(68), 151-158.
- Wittmann, F. H., Roelfstra, P. E. (1980). "Total deformation of loaded drying concrete." *Cem. Concr. Res.*, 10, 601-610.